

JPE 9-4-10

A dP/dV Feedback-Controlled MPPT Method for Photovoltaic Power System Using II-SEPIC

Han-Eol Park* and Joong-Ho Song†

*Dept. of Electric Traction and Signaling System of Railway, Seoul National University of Technology, Korea

†Dept. of Electrical Engineering, Seoul National University of Technology, Korea

ABSTRACT

A dP/dV feedback-controlled MPPT (Maximum Power Point Tracking) method for photovoltaic power systems using II-SEPIC (Isolated Inverse-SEPIC; Single Ended Primary Inductance Converter) is presented and a current-mode dP/dV feedback-controlled MPPT method is devised to apply for the PV power converter system. A control strategy for the current-mode dP/dV feedback control system is developed in this paper and the proposed MPPT shows relatively satisfactory dynamics against rapidly changing insolation conditions. In order to verify the validity and effectiveness of the proposed method, simulations and experiments of the PV power system using II-SEPIC converter are performed. These simulation and experiment results show that the proposed method enables the PV power system to extract maximum power from the photovoltaic module against the solar insolation variation.

Keywords: MPPT, SEPIC, Photovoltaic systems, Current control

1. Introduction

Photovoltaic power systems are comprised of a PV (photovoltaic) cell for converting solar energy into electrical energy and a PCS (Power Conditioning System) for controlling the output power of the cell. PV cells have power-extracting characteristics on generation curves that generally show a single MPP (Maximum Power Point) corresponding to an insolation level and a temperature condition. When the system operates at the MPP, high

efficiency of solar energy conversion is accomplished. Several MPPT (Maximum Power Point Tracking) algorithms to extract more solar energy have been studied. The P&O method, one of the most widely used algorithms, is very simple, but small perturbation of the output voltage appears around the MPP. Consequently, it makes additional power losses and also fails in tracking the MPP under rapidly changing atmospheric conditions. The incremental conductance method, which is another frequently adopted algorithm, is less intricate in implementation and its incremental step size determines how fast the MPP is tracked.

dP/dV feedback-control method is independent of the cell characteristics and can track the MPP very quickly. It can track the real MPP accurately and it responds well to

Manuscript received November 18, 2008; revised May 29, 2009

†Corresponding Author: joongho@snut.ac.kr

Tel: +82-2-970-6415, Fax: +82-2-978-2754,

Dept. of Electrical Engineering, Seoul National University of Technology, Korea

both insolation and temperature variations. Moreover, it needs no PV cell data, pre-experiment or periodic tuning. However, research on the dP/dV feedback-control method has not been done sufficiently because its implementation seems overly complex for high-speed operation^[1]. R. Bhide *et al.* present a MPPT method that varies incremental duty step size according to the signs of dP/dV^[2]. The convergence speed of the method depends on the step size. H. Sugimoto *et al.* study a MPPT approach that uses the dP/dV calculation technique through the linearization-based method^[3]. However, no experimental verification is given for the work results. S. J. Chiang *et al.* show a MPPT method that utilizes sampling and data conversion to calculate the dP/dV value^[4]. Because this method is based on the dynamic characteristics of a PV array obtained only under a stable insolation level, reliability against rapidly changing insolation levels or unstable atmospheric conditions could not been verified.

This paper proposes a dP/dV feedback-controlled MPPT method through direct dP/dV value feedback and brings to PV power generation systems modified dynamic responses with the help of a current-mode dP/dV feedback-controlled MPPT method. The proposed algorithm is implemented on platform consisting of a power circuit of an isolated inverse-SEPIC (II-SEPIC) and a control circuit adopting DSP TMS320F2812. Since II-SEPIC can make wide-range control of input-output voltage conversion and is provided with an isolation transformer, it is suitable as a power converter of the photovoltaic power systems. Validity of the proposed MPPT method is confirmed through simulation and experiment.

2. Description on II-SEPIC

A circuit for a II-SEPIC shown in Fig. 1 can be described along with its operating modes as follows:

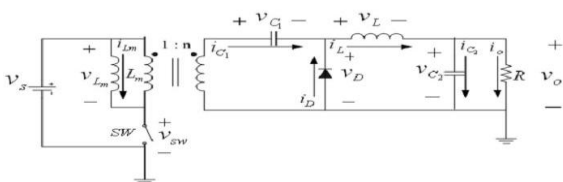


Fig. 1. Circuit of II-SEPIC.

When the switch is closed, the freewheeling diode goes off and the transformer makes a path for supplying power from the input source to the load through the coupling capacitor, with the transformer turn ratio and its polarity considered. When the switch is open, on the other hand, both the coupling capacitor current from a magnetizing inductance current and the filter inductor current flow through the freewheeling diode. The state-space model based on the state-space averaging method is described in the following equation (1)^[5]:

$$\begin{bmatrix} \dot{i}_{L_m} \\ \dot{i}_L \\ \dot{v}_{C_1} \\ \dot{v}_{C_2} \end{bmatrix} = \begin{bmatrix} 0 & 0 & \frac{(1-D)}{nL_m} & 0 \\ 0 & 0 & -\frac{D}{L} & -\frac{1}{L} \\ \frac{(1-D)}{nC_1} & \frac{D}{C_1} & 0 & 0 \\ 0 & \frac{1}{C_2} & 0 & -\frac{1}{RC_2} \end{bmatrix} \begin{bmatrix} i_{L_m} \\ i_L \\ v_{C_1} \\ v_{C_2} \end{bmatrix} + \begin{bmatrix} \frac{D}{L_m} \\ \frac{L}{nD} \\ \frac{L}{L} \\ 0 \end{bmatrix} v_s \quad (1)$$

The DC transfer function under steady state is expressed as:

$$\frac{V_o}{V_s} = n \frac{D}{1-D} \quad (2)$$

It is shown that a II-SEPIC can step-up and step-down the output voltage by the transformer turn ratio and the duty ratio. Through small signal analysis, the control transfer function between the inductor current and the duty ratio can be derived as:

$$\frac{\tilde{i}_L(s)}{\tilde{d}(s)} = \frac{a_3 s^3 + a_2 s^2 + a_1 s + a_0}{b_4 s^3 + b_3 s^2 + b_2 s + b_0} \quad (3)$$

where:

$$a_3 = -\frac{n^3 L_m C_1 C_2 R V_s}{(1-D)}$$

$$a_2 = \frac{n^3 L_m R V_s (C_1 (1-D) - C_2 D^2)}{(1-D)^2}$$

$$a_1 = \frac{n V_s (C_2 R^2 (1-D)^2 - n^2 L_m D^2)}{R(1-D)^2}$$

$$a_0 = n V_s$$

$$b_4 = n^2 L_m L C_1 C_2 R$$

$$b_3 = n^2 L_m L C_1$$

$$b_2 = n^2 L_m R (C_1 + D^2 C_2) + L C_2 R (1-D)^2$$

$$b_1 = n^2 L_m D^2 + L (1-D)^2$$

$$b_0 = R (1-D)^2$$

Fig. 2 shows the root locus of a II-SEPIC which is observed from the current control transfer function.

It is shown in Fig. 2 that two pole-pairs exist in the LHP and that this plant is a non-minimum phase with a zero in the RHP. It is noted from the root locus that the current controller gains should be carefully selected so that all poles exist in the LHP.

3. dP/dV feedback-controlled MPPT method

At first we look into general characteristics of the dP/dV feedback-controlled MPPT method.

Fig. 3 shows a typical characteristic curve for PV cells, in which the dP/dV ratio is zero at the MPP under any insolation or temperature condition. Positioning the dP/dV=0 on the PV cell power-voltage curve in Fig.3 can be implemented by tracking the MPP with the help of the dP/dV slope control loop as shown in Fig. 4.

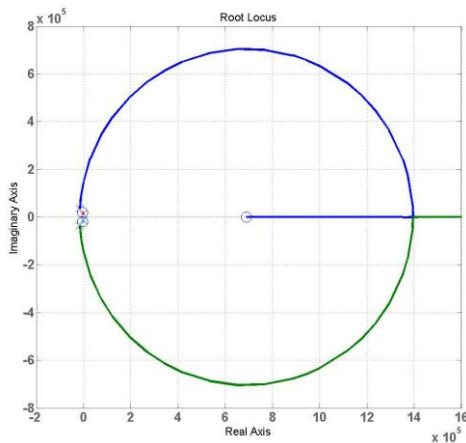


Fig. 2. Root locus for a current control transfer function.

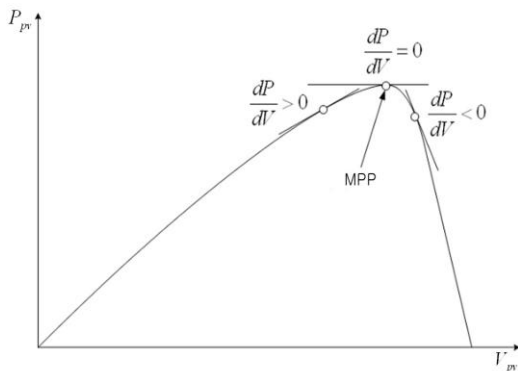


Fig. 3. Maximum power point of a PV cell.

Next, when a PV power system operates at the MPP, the relations among voltages and currents of each component in the converter circuit can be calculated. Assume that PV cells produce output voltage and current corresponding to the MPP. Using the basic equation of PV cells, it can be easily determined that the cell output voltage and the cell output current satisfy a certain relation of equation (4) at the MPP of dP/dV=0^[6].

$$\frac{dP}{dV} = 0 = I_{ph} - I_{sat} \left(e^{\frac{V_m}{V_T}} - 1 \right) - \frac{V_m}{V_T} I_{ph} e^{\frac{V_m}{V_T}} = I_m - \frac{V_m}{V_T} I_{ph} e^{\frac{V_m}{V_T}} \quad (4)$$

In this equation, I_{ph} , I_{sat} and V_T denote the light-generated current, the cell reverse saturation current, and the thermal potential, respectively. V_m and I_m indicate the cell output voltage and the cell output current at the MPP, respectively. Fig. 5(a) shows the typical P-V characteristics of the PV cells against insolation variations. The cell output voltage V_m , and current I_m associated with the MPPs of Fig. 5(a) are plotted in Fig. 5(b).

It is asserted that keeping up the cell output voltage or the cell output current at the MPP values makes the PV cells produce the maximum output power eventually. Assuming no power losses in the converter circuit, a relation between the average output current of the PV cells and the inductor average current can be expressed as follows:

$$V_{PV} I_{PV} = V_o I_o = V_o I_L \quad (5)$$

$$I_{PV} = n \frac{D}{1-D} I_L = k \cdot I_L \quad (6)$$

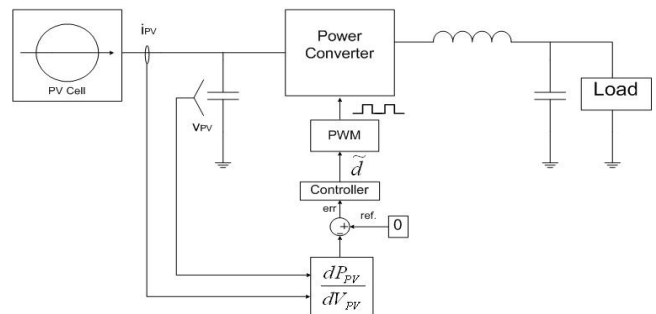


Fig. 4. Functional blocks of a dP/dV feedback-controlled MPPT system.

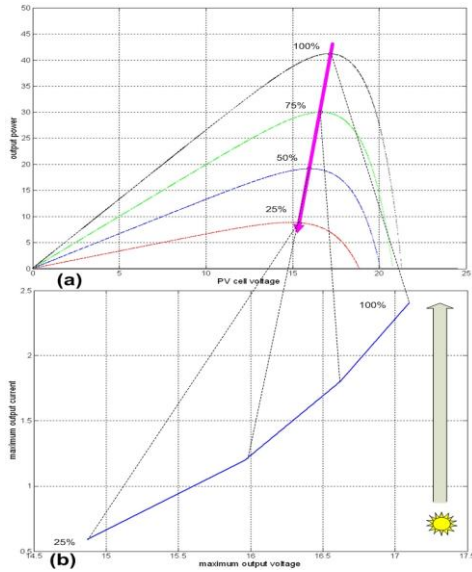


Fig. 5. Relation of maximum output power, voltage, and current. (a) P-V characteristics of PV cells (b) output voltage and current relations along the MPP of PV cells.

In these equations, I_{pv} , I_o and I_L indicate the cell output current, the converter output current and the inductor current, respectively. Eq. (6) shows that the converter inductor current is determined in proportion to the cell output current from Fig. 5(b). It is asserted that there is a linear relation between the cell output current and the converter inductor current under steady state operation. Therefore, controlling the inductor current is equivalent to controlling the PV cell output current.

Current control has many merits. System performance is less sensitive to unwanted disturbances and it can bring over-current protection and improved dynamic responses. If the current control loop is applied in the MPPT control system, it might be useful in effectively controlling the PV parallel-connected power system because it can be treated as a current source. Also, in case of a photovoltaic power system with multi-converters connected to only one battery the current control is more powerful to modularize the whole system than the voltage control^[7].

Fig. 6 shows a PV power system adopting a current-mode dP/dV feedback-controlled MPPT method.

A current controller always controls the inductor current to track the associated current reference. Accordingly, if

the inductor current operating at the MPP is given as the reference of the current controller through the dP/dV feedback-control loop, the MPPT can be achieved. In practical systems, the calculated dP/dV value is compared with its reference and then the resulting error enters the input of the MPP controller. The output signal of the MPP controller is given to the current controller as the inductor current reference. The current controller produces the duty ratio of the converter to track the inductor current reference through proper PWM operation.

4. Simulation results

The PV module used in this paper is the GMS01531 manufactured by LG Industrial Systems and the technical specifications of the PV cell are shown in Table 1.

Table 1. Specifications of the PV cell.

ratings	value
Power(Typical $\pm 10\%$)	53[W]
Current(Typical at Load)	3.05[A]
Voltage (Typical at Load)	17.4[V]
Isc (Typical)	3.35[A]
Voc (Typical)	21.7[V]
1000[W/ m ²], 25[°C], AM 1.5	

The PV module output power-voltage curve measured in the laboratory under twelve 500W halogen lamps is shown in Fig. 7.

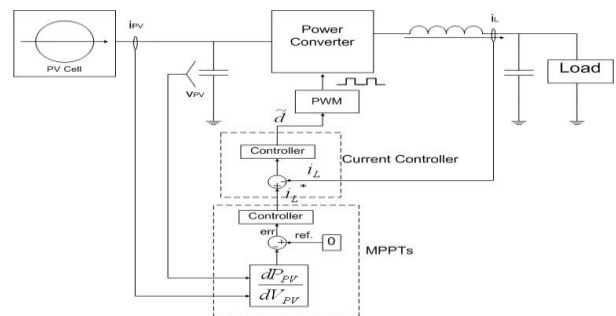


Fig. 6. Control system based on a current-mode dP/dV feedback-controlled MPPT.

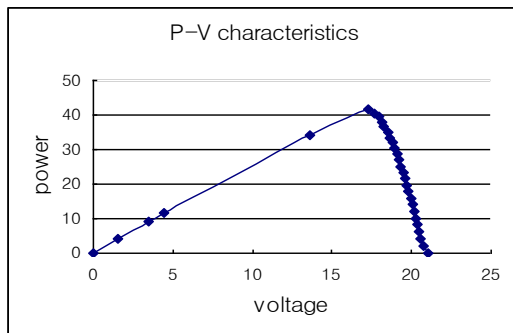


Fig. 7. Output characteristic curve of the PV array.

For simulation and experiment, a II-SEPIC is also designed to comply with the PV module ratings. It is assumed that the inductor current flows in the continuous-current mode and that an adequate input capacitor is chosen to support the output load voltage. The parameters for a II-SEPIC are shown in Table 2.

Table 2. Parameters of a II-SEPIC.

parameter	value
Input capacitor	2000 [uF]
Coupling capacitor	60 [uF]
Filter capacitor	100 [uF]
Inductor	600 [uH]
Switching frequency	20 [kHz]
Transformer turn ratio	1:1

The dP/dV calculation for the MPPT is performed through a discretization process described as:

$$\frac{dP}{dV}(n) = \frac{P(n) - P(n-1)}{V(n) - V(n-1)} \quad (7)$$

Where, $P(n)$ is calculated in the form of $V(n) \cdot I(n)$ and n denotes the n^{th} sampling time. The output characteristics of the photovoltaic power system are predominantly affected by insolation levels. Assuming that the insolation level varies and that the temperature of the PV array is at 25°C, simulations and experiments were performed. Also, in order to verify validity and effectiveness of the dP/dV feedback-controlled MPPT

method, a comparative study with the P&O method is done.

The generated output power using the dP/dV feedback-controlled MPPT method, the current-mode dP/dV feedback-controlled MPPT method and the P&O method is plotted in Fig. 8 and 9, respectively. At 0.05sec, the insolation level changes from a 100% to a 50% rating and then changes up from a 50% to a 100% rating at 0.07sec. It is demonstrated that the dP/dV feedback-controlled MPPT method and the current-mode dP/dV feedback-controlled MPPT method can track the MPP extremely fast. In case of the P&O method, unwanted oscillation appears in the steady-state power response.

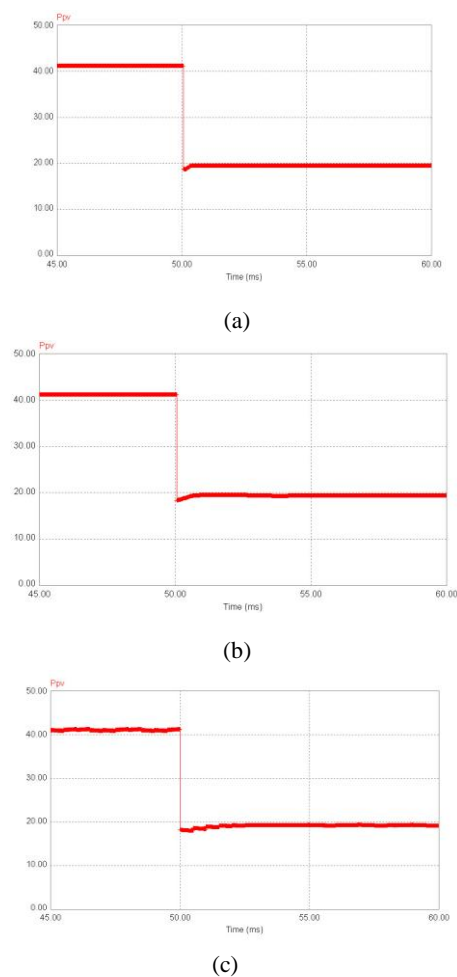


Fig. 8. Generated power trace of the PV module when insolation decreases. (a) dP/dV feedback-controlled MPPT method (b) current-mode dP/dV feedback-controlled MPPT method (c) P&O method.

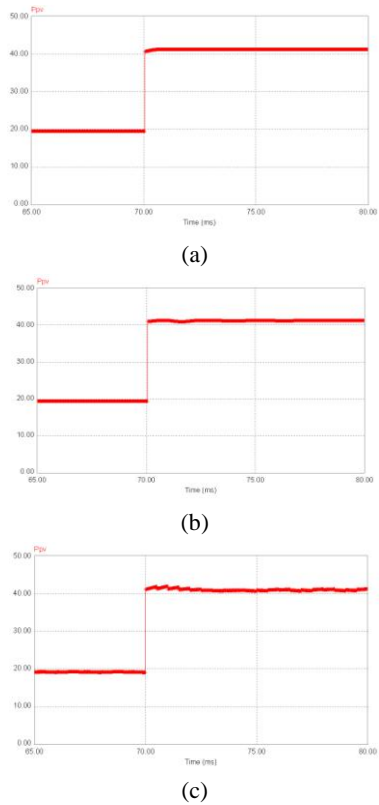


Fig. 9. Generated power trace of the PV module when insolation increases. (a) dP/dV feedback-controlled MPPT method (b) current-mode dP/dV feedback-controlled MPPT method (c) P&O method.

The actual dP/dV value in the closed-loop control system is shown in Fig. 10. It is noted that a good tracking response of the MPPT is obtained since the actual value of dP/dV quickly converges to zero with the help of the dP/dV feedback-controlled MPPT method.

Fig. 11 illustrates how accurately the proposed algorithm can track the MPP on the output power-voltage curve even in case of insolation level changes from 100% to 75%, 50% and 25% respectively. It can be seen in this figure that the dP/dV feedback-controlled MPPT method and the current-mode dP/dV feedback-controlled MPPT method can track the MPP accurately against insolation variations. In the case of the P&O method, oscillations in the generation power appears around the MPP, whereas the dP/dV feedback-controlled MPPT method and the current-mode dP/dV feedback-controlled MPPT method can make the generated power converge stably to the MPP without any oscillation.

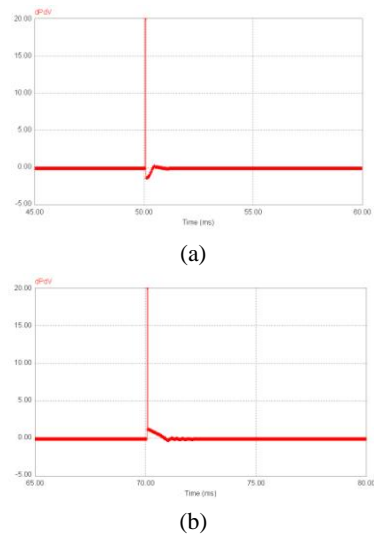


Fig. 10. dP/dV value responses (a) when insolation decreases (b) when insolation increases.

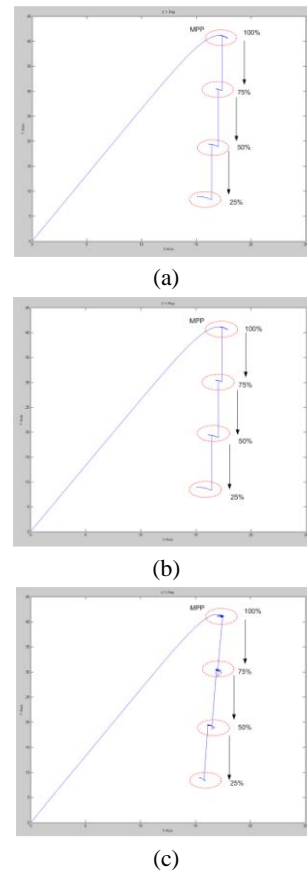


Fig. 11. Output power-voltage curve tracings against varying insolation. (5V/div., 5W/div.) (a) dP/dV feedback-controlled MPPT method (b) current-mode dP/dV feedback-controlled MPPT method (c) P&O method.

5. Experimental results

A prototype of the PV power system is implemented as shown in Fig. 12. dP/dV calculation, a MPPT controller and a current controller are implemented in a TMS320F2812 DSP operating at 150MHz. The sampling frequencies for dP/dV calculation and for current control are selected to be 2kHz and 20kHz, respectively. Also, an anti-windup of the PI controller, an over-current protection and a low pass filter in the data acquisition loop are added^{[8]-[10]}. A LEM LV25-P and a HY5-P are adopted as a voltage and a current transducer respectively, and a PLZ1003W is used as an electronic load. Twelve 500W halogen lamps are used as an artificial illumination to emulate insolation level variations.

The insolation level is defined as 100% insolation when all lamps are on and the level is defined as 50% insolation when half of lamps are off. It is assumed that the PV module operates at room temperature and that electric fans are mounted for cooling and regulating the PV module temperature.

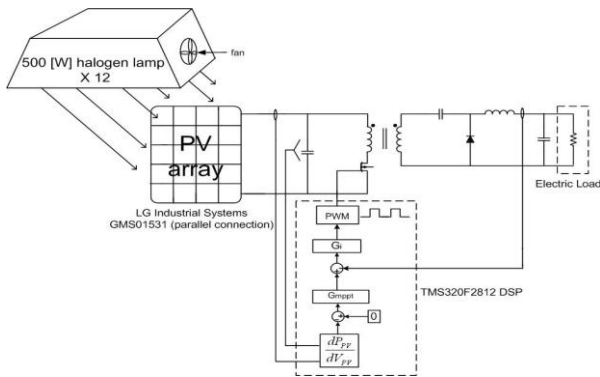


Fig. 12. Experimental setup of the PV power system.

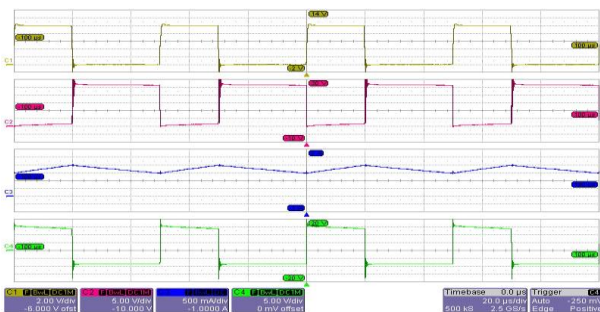


Fig. 13. Experiment waveforms of the II-SEPIC.

Several waveforms of the switching gate signal, the drain-source voltage of the switch, the inductor current and the inductor voltage are captured in the experimental results in Fig. 13.

Fig. 14(a) shows that the dP/dV feedback-controlled MPPT method accomplishes maximum power extraction when the insolation level is changed from 100% to 50% in part A. Similarly, Fig. 14(b) shows that the MPPT is also accomplished when the insolation level is changed from 50% to 100% in part B. The generation power levels shown in Fig. 14 which are obtained through the proposed MPPT coincided with those of Fig. 8 and 9.

Fig. 15(a) shows that the current-mode dP/dV feedback-controlled MPPT method accomplishes maximum power extraction successfully when the insolation level is changed from 100% to 50% in part A. Similarly, Fig. 15(b) shows that the MPPT is also accomplished when insolation level is changed from 50% to 100% in part B. The generation power levels shown in Fig. 15 which are obtained through the proposed MPPT coincide with those of Fig. 8 and 9. By comparing Fig. 15 with Fig. 14, it is claimed that the maximum power tracking responses of the system using the current-mode dP/dV feedback-controlled MPPT method illustrates a smoother transient than those of the dP/dV feedback-controlled MPPT method.

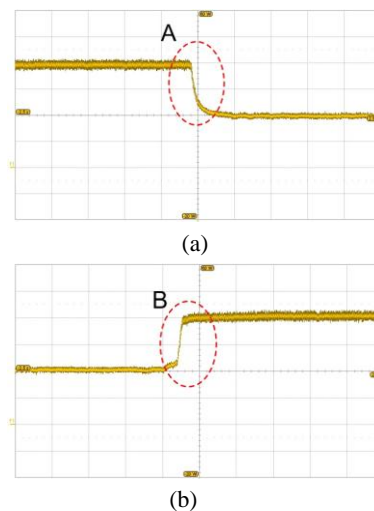


Fig. 14. Output power tracking based on the dP/dV feedback-controlled MPPT method.(500ms/div., 10W/div.): (a) when insolation decreases (b) when insolation increases.

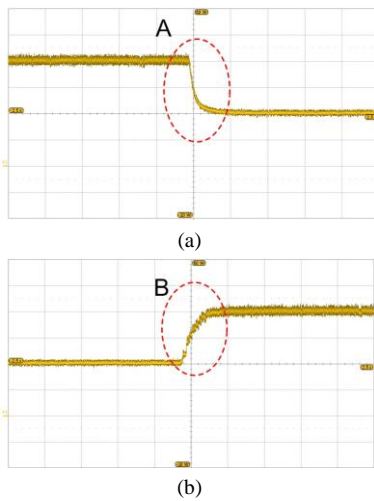


Fig. 15. Output power tracking based on the current-mode dP/dV feedback-controlled MPPT. (500ms/div., 10W/div.) (a) when insolation decreases (b) when insolation increases.

6. Conclusions

In this paper, a dP/dV feedback-controlled MPPT method is devised to extract maximum power from a PV module. Its performance is evaluated both through simulation and experiment. Especially, a current-mode dP/dV feedback-controlled MPPT method for II-SEPIC converters is proposed and a comprehensive study on it is made. The proposed MPPT algorithms illustrate relatively good performances in tracking the maximum power point even when the solar insolation changes abruptly. The experiment shows the validity of the proposed methods and the effectiveness of the PV power system dealt with in this paper.

Acknowledgment

This work is the outcome of a Manpower Development Program for Energy & Resources supported by the Ministry of Knowledge and Economy (MKE)

References

- [1] T. Eswam and P. L. Chapman, "Comparison of photovoltaic array maximum power point tracking techniques," *IEEE Trans. on Energy Conversion*, Vol. 22, No. 2, pp. 439-449, 2007.
- [2] R. Bhide and S. R. Bhat, "Modular power conditioning unit for photovoltaic power tracking control," *in proc. of*

IEEE PESC 1992, pp. 708-713, 1992.

- [3] H. Sugimoto and H. Dong, "A new scheme for maximum photovoltaic power tracking control," *in proc. of IEEE PCC 1997*, pp. 691-696, 1997.
- [4] S. J. Chianq, K. T. Chang, and C. Y. Yen, "Residential photovoltaic energy storage system," *IEEE Trans. on Industrial Electronics*, Vol. 45, No. 3, pp. 385-394, 1998.
- [5] H. E. Park, E. S. Kim and J. H. Song, "Modeling and Control Characteristics of Isolated Inverse-SEPIC," *EPE Journal*, Vol. 18, No. 4, 2008.
- [6] L. Castaner and S. Silvestre, *Modelling Photovoltaic Systems using PSpice*, John Wiley & Sons, 2002.
- [7] C. W. Tan, T. C. Green and C. A. Hernandez-Aramburo, "An improved maximum power point tracking algorithm with current-mode control for photovoltaic applications," *in proc. of IEEE PEDS 2005*, pp. 489-494, 2005.
- [8] Texas Instruments, *TMS320x281x DSP system control and interrupts reference guide: SPRU078D*, Texas Instruments, 2003.
- [9] Texas Instruments, *TMS320x281x DSP analog-to-digital converter (ADC) reference guide: SPRU060D*, Texas Instruments, 2003.
- [10] Texas Instruments, *TMS320x281x DSP event manager (EV) reference guide: SPRU065E*, Texas Instruments, 2003.



Han-Eol Park received B.S. and M.S. degrees in electrical engineering from Seoul National University of Technology, Seoul, Korea, in 2006 and 2008 where he is currently working toward his Ph.D. in electric traction and signaling system of railway. His primary research interests are switching converters, renewable energy systems, and power quality of railway systems.



Joong-Ho Song received B.S. and M.S. degrees in electrical engineering from Seoul National University, Korea in 1980 and 1982, and his Ph.D. from KAIST, Korea, in 1993. He worked as an engineer for E-Hwa Electrical Co., Korea from 1982 to 1985. From 1985 to 2002, he was with the Intelligent System Control Research Center, Korea Institute of Science and Technology. He was a visiting scholar at the University of Wisconsin-Madison from 1995 to 1996. Since 2002, He has been an Associate Professor in the Department of Electrical Engineering at Seoul National University of Technology, Korea. His primary research interests include switching converters, electric machine drives, and renewable energy technologies.